

# Novel quantum transport effects in single-molecule transistors

Felix von Oppen and Jens Koch

Institute for Theoretical Physics, Freie Universität Berlin,  
Arnimallee 14, 14195 Berlin, Germany  
vonoppen@physik.fu-berlin.de, Jens.Koch@physik.fu-berlin.de

**Abstract.** Transport through single molecules differs from transport through more conventional nanostructures such as quantum dots by the coupling to few well-defined vibrational modes. A well-known consequence of this coupling is the appearance of vibrational side bands in the current-voltage characteristics. We have recently shown that the coupling to vibrational modes can lead to new quantum transport effects for two reasons. (i) When vibrational equilibration rates are sufficiently slow, the transport current can drive the molecular vibrations far out of thermal equilibrium. In this regime, we predict for strong electron-phonon coupling that electrons pass the molecule in avalanches of large numbers of electrons. These avalanches consist themselves of smaller avalanches, interrupted by long waiting times, and so on. This self-similar avalanche transport is reflected in exceptionally large current (shot) noise, as measured by the Fano factor, as well as a power-law frequency spectrum of the noise. (ii) Due to polaronic energy shifts, the effective charging energy of molecules may be strongly reduced compared to the pure Coulomb charging energy. In fact, for certain molecules the effective charging energy  $U$  can become negative, a phenomenon known in chemistry as potential inversion. We predict that transport through such negative- $U$  molecules near charge-degeneracy points, where the Coulomb blockade is lifted, is dominated by tunneling of electron pairs. We show that the dependence of the corresponding Coulomb-blockade peaks on temperature and bias voltage is characteristic of the reduced phase space for pair tunneling.

## 1 Sketch of molecular electronics

In recent years, electronic transport through nanostructures has witnessed a shift towards molecular systems [1, 2]. Several ingenious schemes for measuring transport through single molecules have been realized and experimental control over such systems is rapidly improving. The most popular experimental techniques create two closely spaced (gold) electrodes by the use of breakjunctions [3, 4, 5] or electromigration [6]. The molecule may or may not be chemically bound (e.g. by thiol groups) to the electrodes. An alternative method first attaches the molecule to gold clusters via thiol groups before maneuvering (using ac-fields) the resulting conglomerate towards two micro-fabricated electrodes [7]. An intriguing direction is the use of wet molecular junctions, where the molecule is immersed in an electrolytic environment [8].

Another powerful method employs a scanning-tunneling-microscope (STM) tip as an electrode for measuring the current through a molecule, which rests on a substrate [9].

Experiments on single-molecule junctions observe many effects familiar from conventional nanostructures such as quantum dots, especially in setups that include a gate electrode. Prominent examples are the Coulomb blockade which arises due to the large charging energy of nanostructures, as well as the Kondo effect [10]. Due to the small size of molecules, the Kondo effect persists in these systems to rather high temperatures [11]. It has been argued that Coulomb-blockade physics, via charging fluctuations of nearby traps, is also at the origin of temporal fluctuations in the measured  $IV$  characteristics [7].

A prime difference between transport through single molecules as opposed to transport through more conventional nanostructures lies in the coupling of the electronic degrees of freedom responsible for transport to few well-defined vibrational modes (phonons). A prominent effect of this electron-phonon coupling is the appearance of vibrational sidebands in the current-voltage characteristics. These are observed at large bias voltages, comparable to or larger than typical phonon frequencies. While the basic phenomenon has been known for a number of decades [12, 13, 14], current interest in the context of single-molecule junctions started with the work of Park *et al.* [15] on a  $C_{60}$  molecule located in between two metallic leads.

In the meantime, vibrational features have been observed in transport in a wide variety of molecules, ranging from hydrogen  $H_2$  [16] to larger conjugated molecules [9]. Depending on the system, vibrations appear in the current-voltage ( $IV$ ) characteristics as steps or kinks [17]. Typically, molecules more strongly coupled to the leads (as for example in STM experiments where the molecule is lying on the substrate) will exhibit kinks in the  $IV$  characteristics [9]. By contrast, steps in the  $IV$  characteristic are observed for weakly coupled molecules (as for example in breakjunction experiments without chemical bond between electrode and molecule) [15].

An important parameter in single-molecule junctions is the vibrational relaxation rate. For some systems, relaxation times can be as large as 10ns (measured for suspended nanotubes) [18]. Thus, these times can be comparable or longer than the time between two consecutive electrons traversing the molecule which are of the order of 100ps (0.1ps) for a current of 1nA ( $1\mu A$ ). Thus, in the intriguing regime of slow vibrational relaxation (large currents), the current drives the molecular vibrations far out of equilibrium [19, 20]. Such nonequilibrium vibrations have so far been observed directly in at least one experiment as *absorption* satellites of Coulomb blockade peaks [18].

The theoretical description of transport through single molecules rests on two pillars which are at present somewhat disconnected. One approach uses density functional theory to obtain a detailed account of the molecular orbitals including parts of the electrodes [21]. In a second step, the Kohn-Sham

potentials of density functional theory are used to set up a (single-particle) transport problem in the spirit of Landauer. While there are impressive successes, differences between experiment and this “ab-initio” theory can be as large as several orders of magnitude [22]. Discrepancies between theory and experiment are particularly pronounced for fully conjugated molecules. It is important to realize that the use of density-functional theory for transport is an uncontrolled (though often useful) approximation as there is no theorem underlying the definition of a scattering problem on the basis of the Kohn-Sham orbitals. There are some efforts under way to improve this situation within the context of time-dependent density functional theory [23, 24]. It is also difficult to account for the coupling to molecular vibrations as well as electronic correlations within density functional theory.

An alternative approach starts from models of electronic transport through nanostructures [25, 19]. This approach finds its justification in the fact that experiments on molecular junctions exhibit several phenomena which are familiar from quantum dots. In addition, such models can in principle be treated systematically in a variety of transport regimes, including the coupling to molecular vibrations and electronic correlation effects. A minimal model assumes that transport through the molecule is dominated by a single, spin-degenerate molecular orbital  $\varepsilon_d$  [lowest unoccupied molecular orbital (LUMO) or highest occupied molecular orbital (HOMO)], coupled to one vibrational mode of frequency  $\omega$ . Double occupation of the molecular orbital “costs” a charging energy  $U$ . Adding electrons to the molecule shifts the equilibrium position of the nuclei, which provides a coupling of the electronic and vibrational degrees of freedom of the molecule. This physics is sketched in Fig. 1 and encapsulated in the Hamiltonian [13, 14, 19]

$$H = H_{\text{mol}} + H_{\text{vib}} + H_{\text{leads}} + H_{\text{i}}, \quad (1)$$

where the separate contributions correspond to the electronic molecular orbital

$$H_{\text{mol}} = \varepsilon_d n_d + U n_{d\uparrow} n_{d\downarrow}, \quad (2)$$

to the molecular vibrations

$$H_{\text{vib}} = \hbar\omega b^\dagger b + \lambda\hbar\omega(b^\dagger + b)n_d, \quad (3)$$

to the leads

$$H_{\text{leads}} = \sum_{a=L,R} \sum_{\mathbf{p},\sigma} \epsilon_{\mathbf{p}} c_{a\mathbf{p}\sigma}^\dagger c_{a\mathbf{p}\sigma}, \quad (4)$$

and to the tunneling between leads and molecule,

$$H_{\text{i}} = \sum_{a=L,R} \sum_{\mathbf{p},\sigma} (t_a c_{a\mathbf{p}\sigma}^\dagger d_\sigma + \text{h.c.}). \quad (5)$$

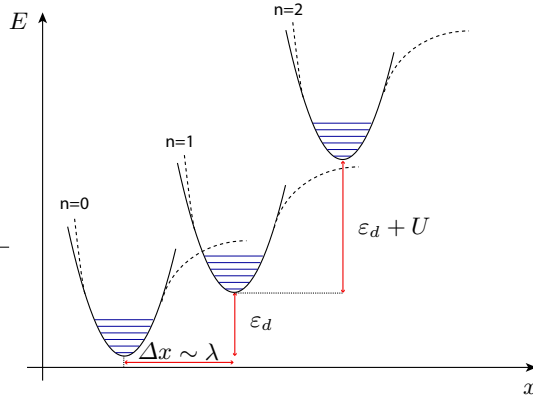


**Fig. 1.** Potential surfaces corresponding to the model Hamiltonian of a molecule featuring a single, spin-degenerate electronic orbital coupled to a single vibrational mode. The model Hamiltonian approximates the potential surfaces by a harmonic-oscillator potential.

Here, the operator  $d_\sigma$  annihilates an electron with spin  $\sigma$  on the molecule,  $c_{a\mathbf{p}\sigma}$  annihilates an electron in lead  $a$  ( $a = L, R$ ) with momentum  $\mathbf{p}$  and spin  $\sigma$ , vibrational excitations are annihilated by  $b$ , and  $t_{L,R}$  denotes the tunneling matrix elements. The electron-phonon coupling (with coupling constant  $\lambda$ ) can be eliminated by the Lang-Firsov canonical transformation [26], which implies renormalizations of the tunneling Hamiltonian  $t_a \rightarrow t_a e^{-\lambda(b^\dagger - b)}$ , of the orbital energy  $\varepsilon_d \rightarrow \varepsilon_d - \lambda^2 \hbar\omega$ , and of the charging energy  $U \rightarrow U - 2\lambda^2 \hbar\omega$ .

Frequently, the position of the molecular orbital  $\varepsilon_d$  can be varied experimentally by a gate voltage. Electronic transport proceeds by a variety of processes, depending on the position of  $\varepsilon_d$  relative to the Fermi energies of the leads. If  $\varepsilon_d$  lies within the bias voltage window between the Fermi energies of left and right lead, transport occurs by sequential (or resonant) tunneling. On the other hand, electrons will occupy the molecule only virtually while tunneling between left and right lead, if the molecular orbital lies far below or far above this bias-voltage window. The latter process is often referred to as cotunneling in the quantum-dot literature [27].

In the limit of high temperatures (as compared to the molecule-lead coupling), transport through single molecules can be treated systematically within the rate-equation approach [28, 29, 19]. Rate equations allow one to account for the coupling to molecular vibrations, for charging effects, as well as for the spin degrees of freedom. This approach has been successfully employed in the theory of vibrational sidebands [25, 19, 30], in describing transport through magnetic molecules [31], as well as in the description of the regime of vibrational nonequilibrium mentioned above [20].

Beyond the rate-equation limit, no systematic theoretical methods are currently available, when charging effects are relevant. An exception is the theory of Kondo correlations where vibrational sidebands of the Kondo resonance have been predicted [32]. Effects of the charging energy  $U$  are less prominent if the molecule is well coupled to at least one of the electrodes, as e.g., in most STM experiments. In this case the time spent by the electron on the molecule is small compared to the inverse phonon frequency, and one expects that perturbation theory in the electron-phonon coupling is appropriate [33].

While experiments to date, with few exceptions, have focused on measurements of  $IV$  characteristics, a number of other quantities have been investigated theoretically. A very interesting quantity is shot noise in the transport current which has been widely investigated in the context of conventional nanostructures, both in theory and experiment [34]. It has been shown that vibrational sidebands also appear in the noise power as function of bias voltage [19, 30], and giant shot noise has been predicted in certain situations of vibrational nonequilibrium (see Sec. 3) [30, 35]. Thermoelectric and thermal properties of molecular junctions were studied theoretically in several works [36, 37, 38]. A particularly interesting quantity is the thermopower which, unlike the  $IV$  characteristic, would give information on whether the current flow proceeds predominantly through LUMO or HOMO. The underlying reason is that a nonzero thermopower requires breaking of particle-hole symmetry about the Fermi energy.

## 2 Novel quantum transport effects

As mentioned above, transport experiments on single-molecule transistors exhibit effects familiar from transport through quantum dots, most notably the Coulomb blockade as well as the Kondo effect. In view of this, it is natural and important to ask the following question: Can we exploit the enormous variety of molecular structures to observe novel quantum transport effects or to access novel regimes of quantum transport? This question is particularly pertinent to those of us, who prefer to approach molecular electronics as a field of science rather than engineering.

A natural place to look for such novel transport physics in single-molecule transistors involves the coupling of the current-carrying electrons to the molecular vibrations. The reason is that unlike quantum dots, where one would be typically dealing with an entire continuum of phonon modes, molecules typically have few well-defined and localized vibrational modes. Indeed, we believe that there are at least two reasons why this coupling to molecular vibrations can lead to novel quantum transport which goes beyond the vibrational side bands reviewed in the previous section.

The first reason is that the transport current can drive the molecular vibrations far out of thermal equilibrium. We will review in Sec. 3 below that

this may result in self-similar avalanche transport. The second reason is the polaronic downward renormalization of the charging energy  $U \rightarrow U - 2\lambda^2 \hbar\omega$  mentioned in Sec. 1. The renormalization is particularly intriguing when the effective charging energy becomes negative. This situation is familiar from negative- $U$  centers in semiconductors and referred to as potential inversion in electrochemistry. We show in Sec. 4 that transport in this regime is characterized by pair tunneling of electrons.

### 3 Franck-Condon blockade and self-similar avalanche transport

In the high-temperature limit, the tunneling Hamiltonian  $H_1$  may be treated perturbatively, and the formalism of rate equations can be employed for the computation of current and noise [28, 29, 19]. The central input to this formalism consists of the rates for the tunneling-induced transitions, which can be obtained systematically by an expansion of the  $T$ -matrix and the use of Fermi's golden rule. Due to the presence of electron-phonon coupling, all electronic transitions are accompanied by transitions in the space of molecular vibrations. In the transition rates, this is reflected by Franck-Condon (FC) matrix elements which are given by the overlap of the initial and final harmonic-oscillator wavefunction. As depicted in Fig. 2, the FC matrix elements crucially depend on the strength of the electron-phonon coupling.

Strong electron-phonon coupling ( $\lambda \gg 1$ ) is characterized by a large displacement between the molecular potential surfaces for different charge states. As a result, the overlap between vibrational states in the vicinity of the ground state acquire an exponential suppression, and the corresponding FC matrix elements are drastically reduced for low-lying phonon states, see Fig. 2. At low bias voltages where only vibrational states close to the ground states are accessible, this reduction of FC matrix elements causes a strong current suppression which we termed *Franck-Condon blockade* [30]. In contrast to other current suppressions such as Coulomb blockade, the FC blockade cannot be lifted by tuning a gate voltage. This provides a characteristic fingerprint that may be accessed in experiments with gated setups.

The FC blockade is a generic feature for strong electron-phonon coupling, independent of the vibrational relaxation rate. Surprisingly however, the transport mechanisms for strong and weak vibrational relaxation are entirely different. For strong vibrational relaxation, the occupation of vibrational states is fixed to the thermal equilibrium distribution. When applying a bias, electrons are transferred across the molecule one by one, and the current shot noise is sub-Poissonian, as usually expected in the case of transport by fermionic carriers. By contrast, for weak vibrational relaxation it is the tunneling dynamics which determines the phonon distribution. We have shown that the vibrational nonequilibrium causes *avalanches* of large numbers of electrons intermitted by long waiting times [30, 35], see Fig. 3. The

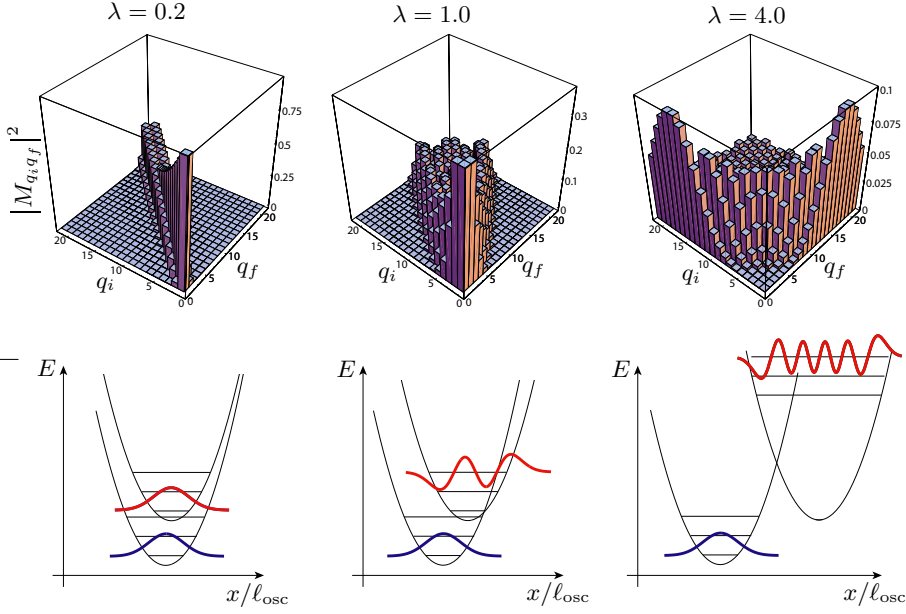


**Fig. 2.** Franck-Condon matrix elements for weak ( $\lambda = 0.2$ ), intermediate ( $\lambda = 1$ ), and strong ( $\lambda = 4$ ) electron-phonon coupling. The upper panel depicts the squared Franck-Condon matrix elements as a function of initial and final phonon states,  $q_i$  and  $q_f$ . The lower panel illustrates the corresponding shifts  $\Delta x = \sqrt{2}\lambda\ell_{\text{osc}}$  of the harmonic oscillator potentials for the two charge states  $n = 0$  and  $n = 1$ .

corresponding shot noise is drastically enhanced ( $F \sim 10^2\text{--}10^3$  for  $\lambda = 4$ ), where the Fano factor reflects the average number of electrons per avalanche.

The origin of these avalanches can be traced back to the increase of the FC matrix elements towards highly excited phonon states, and to the fact that weak vibrational relaxation allows for the accumulation of phonon excitations. As a concrete example, we consider the situation of a low bias voltage that limits the maximal number of phonon excitations to  $\Delta q = 1$  per tunneling event. Then, long waiting times always occur whenever the system resides in the vibrational ground state. When the system succeeds in making a transition, the increase of FC matrix elements towards higher phonon numbers will favor the excitation of one phonon. The accessible transition rates from the state  $q = 1$  are significantly larger due to the enhanced overlap of harmonic-oscillator wavefunctions. Consequently, the system undergoes a rapid series of tunneling events, proceeding to even higher phonon excitations. This dynamics forms an avalanche, which is only terminated when by chance, the system returns to the vibrational ground state.

Zooming into one such avalanche, we have shown that it consists of smaller avalanches, see Fig. 3. This *self-similarity* is explained by the fact that the situation in the first excited phonon state  $q = 1$  very much resembles the

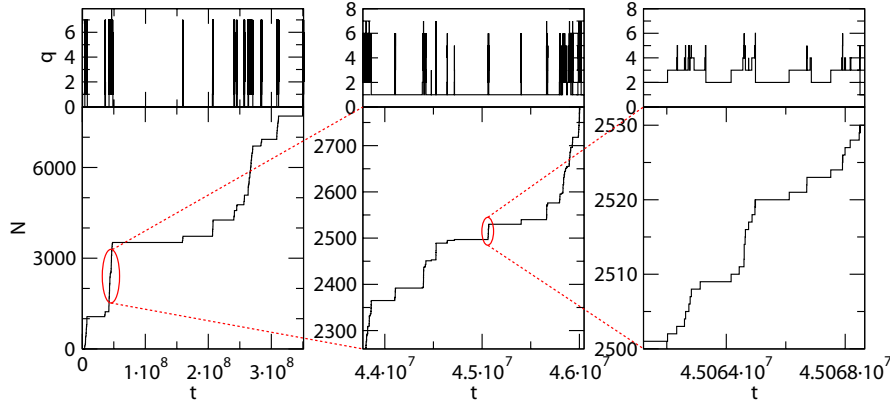


**Fig. 3.** Self-similar electron avalanches for strong electron-phonon coupling ( $\lambda = 4.5$ ). The lower three panels depict the number of transferred electrons  $N$  as a function of time  $t$  (in units of  $\hbar/\Gamma$ ). The middle and right hand plot are magnifications of the respective previous plot, resolving the self-similar structure. The upper panels depict the number  $q$  of excited phonons, revealing that waiting times of different hierarchy levels correspond to different  $qs$ .

ground state situation: Again, the transition rates for  $q = 1$  are suppressed and increase when reaching higher phonon levels, resulting in waiting times and (sub-)avalanches. Experimentally, this self-similarity may be probed by a measurement of the noise frequency spectrum, which exhibits a characteristic power-law decay as a function of frequency,  $S \sim f^{-1/2}$ . Interestingly, the self-similar nature of the avalanches allows for a completely analytical treatment of the transport, and the derivation of a compact formula for the Fano factor as well as the full counting statistics [35].

## 4 Negative- $U$ molecules

Apart from the emergence of FC matrix elements in transition rates, the coupling between electronic and vibrational degrees of freedom also leads to a renormalization of the charging energy  $U \rightarrow U - 2\lambda^2\hbar\omega$ , the *polaron shift*. The most intriguing consequence of this downward shift is the possibility of a negative charging energy, i.e. an effectively attractive electron-electron interaction. In electrochemistry, examples for this scenario are in fact known [41]. Negative  $U$  causes the system to favor even occupation numbers, and by tuning the gate voltage the charge states  $n = 0$  and  $n = 2$  can become degenerate.

At very low temperatures, this scenario leads to the charge Kondo effect [42], and several papers have recently investigated this regime numerically [43, 44]. In the high-temperature regime  $T \gg T_K$ , Kondo correlations are

irrelevant up to logarithmic corrections. We have shown that in this limit transport in the negative- $U$  model is dominated by tunneling of electron *pairs* [45]. In distinction to sequential tunneling and elastic cotunneling, this two-particle process is associated with a reduced phase space, resulting in a characteristically different behavior of the corresponding rates. While sequential and elastic cotunneling lead to constant rates [whenever the one-particle level is located in the bias window], pair-tunneling rates increase roughly linearly with the detuning  $\varepsilon_d + U/2$  of the two-particle level below the lead Fermi energy.

At the degeneracy point  $2\varepsilon_d + U = 0$ , the tunneling of electron pairs generates a peak in the linear conductance as a function of gate voltage. As a result of the linear increase of rates with detuning, the peak width is proportional to temperature while its height is fixed to  $G = 24e^2\Gamma_L\Gamma_R/U^2h$ , where  $\Gamma_a = 2\pi\nu|t_a|^2$  denotes the partial level width induced by tunneling in junction  $a$ . It is important to note that this scaling of the peak with temperature is entirely different from the conventional Coulomb-blockade peak, for which peak height and width are correlated so that its integral value remains constant.

Additional differences between the conventional Coulomb blockade and the negative- $U$  scenario emerge at finite bias. Apart from the cotunneling regime, the nonlinear  $IV$  characteristics for negative  $U$  show regions dominated by pair tunneling. In contrast to conventional Coulomb diamonds, inside which the current is essentially constant, the pair-tunneling regions are signalled by a phase-space induced current increase with growing bias voltage.

Intriguingly, the realistic scenario of coupling asymmetry,  $\Gamma_L \neq \Gamma_R$  causes a negative- $U$  device to develop transistor-like properties. Specifically, we have shown that for  $\Gamma_L \ll \Gamma_R$  the current strongly depends on the bias direction, resulting in *current rectification*. Additionally, the sense of rectification may be altered by the gate voltage, allowing for a *gate-controlled switching* of the device. We have explained this behavior in terms of the dominant transport mechanism for asymmetric coupling, which involves a transition with an electron pair leaving to (or coming from) opposite leads. It is the gate-voltage dependence of such a process that results in the transistor-like behavior.

## 5 Summary

We have shown that single-molecule transistors are a promising arena for novel quantum transport physics for at least two reasons. First, the current can drive the molecular vibrations far out of thermal equilibrium. We find that in the regime of strong electron-phonon interaction, this may lead to current flow in the form of a self-similar hierarchy of avalanches of large numbers of electrons. Specifically, this effect occurs in a regime of transport

which we term Franck-Condon blockade where the low-bias current is suppressed due to the coupling to vibrational modes, even when the molecular orbital is located in the bias-voltage window between the Fermi energies of the two leads. Experimental signatures of self-similar avalanche transport are giant Fano factors, a power-law shot noise spectrum, as well as strongly non-Gaussian full counting statistics. We also mention in passing that interesting non-equilibrium effects occur for weak electron-phonon interactions where the degree of vibrational nonequilibrium grows as the electron-phonon interaction decreases. Vibrational nonequilibrium may also affect vibrational sidebands for anharmonic or charge-dependent molecular vibrations [39, 40].

Second, the coupling to vibrations renormalizes the molecular charging energy by a polaronic energy shift. As familiar from the theory of superconductivity, the electron-phonon interaction counteracts the Coulomb repulsion and reduces the effective charging energy of the molecule. This downward renormalization of the charging energy becomes particularly interesting when the resulting effective charging energy becomes negative. In this case, the molecular ground states as function of gate voltage always involves an even number of electrons. We have shown that transport through such negative- $U$  molecules is dominated by tunneling of electron pairs near those gate voltages where two molecular charge states become degenerate. The corresponding Coulomb blockade peaks directly reflect the characteristic phase space for pair tunneling, which provides convenient experimental signatures of pair tunneling.

The work reviewed in this paper has been supported by Sfb 658 and the Studienstiftung d. dt. Volkes. We have benefitted from discussions with many colleagues. We would like to mention specifically A. Nitzan, Y. Oreg, M. Raikh, E. Sela, as well as M. Semmelhack, with whom we have collaborated on various aspects of molecular electronics.

## References

1. M. A. Reed and J. M. Tour, *Scientific American* **282**, 86 (2000).
2. C. Joachim, J. K. Gimzewski, and A. Aviram, *Nature (London)* **408**, 541 (2000).
3. J. Moreland and J. W. Ekin, *J. Appl. Phys.* **58**, 3888 (1985).
4. C. Zhou, C. J. Muller, M. R. Deshpande, J. W. Sleight, and M. A. Reed, *Appl. Phys. Lett.* **67**, 1160 (1995).
5. J. M. van Ruitenbeek, A. Alvarez, I. Piñeyro, C. Grahmann, P. Joyez, M. H. Devoret, D. Esteve, and C. Urbina, *Rev. Sci. Instrum.* **67**, 108 (1996).
6. H. Park, A. K. L. Lim, A. P. Alivisatos, J. Park, and P. L. McEuen, *Appl. Phys. Lett.* **75**, 301 (1999).
7. T. Dadoosh, Y. Gordin, R. Krahne, I. Khivrich, D. Mahalu, V. Frydman, J. Sperling, A. Yacoby, and I. Bar-Joseph, *Nature (London)* **436**, 677 (2005).
8. L. Grüter, F. Cheng, T. T. Heikkilä, M. T. Gonzalez, F. Diederich, C. Schönenberger, and M. Calame, *Nanotechnology* **16**, 2143 (2005).

9. X. H. Qiu, G. V. Nazin, and W. Ho, Phys. Rev. Lett. **92**, 206102 (2004).
10. J. Park, A. N. Pasupathy, J. I. Goldsmith, C. Chang, Y. Yaish, J. R. Petta, M. Rinkoski, J. P. Sethna, H. D. Abruñas, P. L. McEuen, and D. C. Ralph, Nature (London) **417**, 722 (2002).
11. L. H. Yu and D. Natelson, Nano Lett. **4**, 79 (2004).
12. R. C. Jaklevic and J. Lambe, Phys. Rev. Lett. **17**, 1139 (1966).
13. L. I. Glazman and R. I. Shekhter, Sov. Phys. JETP **67**, 163 (1988).
14. N. S. Wingreen, K. W. Jacobsen, and J. W. Wilkins, Phys. Rev. Lett. **61**, 1396 (1988).
15. H. Park, J. Park, A. K. L. Lim, E. H. Anderson, A. P. Alivisatos, and P. L. McEuen, Nature **407**, 57 (2000).
16. R. H. M. Smit, Y. Noat, C. Untiedt, N. D. Lang, M. C. van Hemert, and J. M. van Ruitenbeek, Nature **419**, 906 (2002).
17. M. Galperin, M. A. Ratner, and A. Nitzan, J. Chem. Phys. **121**, 11965 (2004).
18. B. LeRoy, S. Lemay, J. Kong, and C. Dekker, Nature **432**, 371 (2004).
19. A. Mitra, I. Aleiner, and A. J. Millis, Phys. Rev. B **69**, 245302 (2004).
20. J. Koch, M. Semmelhack, F. von Oppen, and A. Nitzan, Phys. Rev. B **73**, 155306 (2006).
21. Y. Xue and M. A. Ratner, Phys. Rev. B **68**, 115407 (2003).
22. F. Evers, F. Weigend, and M. Koentopp, Phys. Rev. B **69**, 235411 (2004).
23. K. Burke, R. Car, and R. Gebauer, cond-mat/0410352 (2004).
24. S. Kurth, G. Stefanucci, C.-O. Almbladh, A. Rubio, and E. K. U. Gross, Phys. Rev. B **72**, 035308 (2005).
25. S. Braig and K. Flensberg, Phys. Rev. B **68**, 205324 (2003).
26. I. G. Lang and Y. A. Firsov, Sov. Phys. JETP **16**, 1301 (1963).
27. H. Grabert and M. H. Devoret, eds., *Single Charge Tunneling in Coulomb Blockade Phenomena in Nanostructures* (Plenum Press, New York and London, 1992).
28. C. W. J. Beenakker, Phys. Rev. B **44** (1646).
29. D. V. Averin, A. N. Korotkov, and K. K. Likharev, Phys. Rev. B **44**, 6199 (1991).
30. J. Koch and F. von Oppen, Phys. Rev. Lett. **94**, 206804 (2005).
31. F. Elste and C. Timm, Phys. Rev. B **71**, 155403 (2005).
32. J. Paaske and K. Flensberg, Phys. Rev. Lett. **94**, 176801 (2005).
33. S. Gao, M. Persson, and B. I. Lundqvist, Phys. Rev. B **55**, 4825 (1997).
34. Y. M. Blanter and M. Büttiker, Phys. Rep. **336**, 1 (2000).
35. J. Koch, M. E. Raikh, and F. von Oppen, Phys. Rev. Lett. **95**, 056801 (2005).
36. D. Segal and A. Nitzan, J. Chem. Phys. **117**, 3915 (2002).
37. D. Segal, A. Nitzan, and P. Hänggi, J. Chem. Phys. **119**, 6840 (2003).
38. J. Koch, F. von Oppen, Y. Oreg, and E. Sela, Phys. Rev. B **70**, 195107 (2004).
39. J. Koch and F. von Oppen, Phys. Rev. B **72**, 113308 (2005).
40. M. R. Wegewijs and K. C. Nowack, New J. Phys. **7**, 239 (2005).
41. C. Kraiya and D. H. Evans, J. Electroanal. Chem. **565**, 29 (2004), and references therein.
42. A. Taraphder and P. Coleman, Phys. Rev. Lett. **66**, 2814 (1991).
43. P. S. Cornaglia, H. Ness, and D. R. Grempel, Phys. Rev. Lett. **93**, 147201 (2004).
44. L. Arrachea and M. J. Rozenberg, Phys. Rev. B **72**, 041301(R) (2005).

12 Felix von Oppen and Jens Koch

45. J. Koch, M. E. Raikh, and F. von Oppen, Phys. Rev. Lett. **96**, 056803 (2006).